

# Combined sparsifying transforms for compressed sensing MRI

X. Qu, X. Cao, D. Guo, C. Hu and Z. Chen

In traditional compressed sensing MRI methods, single sparsifying transform limits the reconstruction quality because it cannot sparsely represent all types of image features. Based on the principle of basis pursuit, a method that combines sparsifying transforms to improve the sparsity of images is proposed. Simulation results demonstrate that the proposed method can well recover different types of image features and can be easily associated with total variation.

**Introduction:** Recently emerged compressed sensing (CS) [1,2] provides a firm foundation to reconstruct a signal from incomplete measurements assuming the signal can be sparsely represented by certain transform. CS was first applied in MRI in [3] and the result is very impressive. Sparsity of images limits the quality of a reconstructed image for compressing sensing MRI (CS-MRI) [1–3]. A traditional 2-D wavelet was employed to sparsify magnetic resonance (MR) images [3]. The wavelet is good at sparsely representing point-like features but fails in sparsely representing curve-like features. New tailored geometric transforms such as curvelet [4] and contourlet [5,6] can be used to sparsely represent curves. However, neither is good at representing point-like image features. So far, how to exploit multiple geometric transforms to improve the sparsity of MR images for CS reconstruction has not been discussed. This Letter presents a new method to combine these transforms for CS-MRI and improve the quality of reconstructed images.

**Theory:** As a major approach to solve CS, basis pursuit [7] suggests improving the sparsity of signal  $x$  with length  $N$  in overcomplete waveform dictionaries  $\Psi = [\Psi_1, \Psi_2, \dots, \Psi_j, \dots, \Psi_M]^T$  ( $M > N$ ) and finding the sparsest representation by solving the  $l_1$  minimisation problem. Each waveform  $\Psi_j$  is a row vector with length  $N$ . Then coefficients  $\alpha_{M \times 1} = \Psi_{M \times N} x_{N \times 1}$  and each entry  $\alpha_j$  is the inner product  $\langle \Psi_j, x \rangle$ . The MR image can be reconstructed from undersampled k-space data via finding a solution to

$$\arg \min_x \|\alpha\|_1 \quad \text{subject to} \quad F_u x = y \quad (1)$$

where  $\|\alpha\|_1 = \sum_{j=1}^M |\alpha_j| = \sum_{j=1}^M |\langle \Psi_j, x \rangle|$ ,  $F_u$  is the undersampling Fourier operator and  $y$  is the acquired incomplete k-space data.

We view  $[\Psi_1, \Psi_2, \dots, \Psi_j, \dots, \Psi_M]$  as concatenation of the subsets  $\{\psi_{\Lambda_i}, i = 1, 2, \dots, I\}$ , where  $\Lambda_i$  is the indices of waveforms in the  $i$ th subset. Since  $l_1$  norm is a separable function,  $\|\alpha\|_1$  can be calculated as

$$\|\alpha\|_1 = \sum_{j=1}^M |\langle \Psi_j, x \rangle| = \sum_{i=1}^I \sum_{j \in \Lambda_i} |\langle \Psi_j, x \rangle| = \sum_{i=1}^I \|\langle \psi_{\Lambda_i}, x \rangle\|_1 \quad (2)$$

This indicates that  $l_1$  norm minimisation in the global overcomplete dictionary is equivalent to minimising the sum of  $l_1$  norm of the dictionary's subsets. So, (1) can be written as

$$\arg \min_x \sum_{i=1}^I \|\langle \psi_{\Lambda_i}, x \rangle\|_1 \quad \text{subject to} \quad F_u x = y \quad (3)$$

This provides us with an opportunity to recover the MR image from the union of subsets of the waveform's dictionary. In this Letter, we consider each union of subsets  $\psi_{\Lambda_i}$  comes from commonly used transforms which sparsify different types of image features. Because these subsets are complementary to give sparse representation of image features, sparsity of image can be improved according to basis pursuit [7]. However, it is hard to explicitly show the waveforms of frame-based transform, e.g. curvelet and contourlet. Furthermore, storing and computation of  $\alpha$  is expensive because the dimension of  $\alpha$  is higher than the dimension of signal  $x$  for the overcomplete dictionary. Instead, we can apply fast forward transform  $T_i$  on the image and get another version of (3):

$$\arg \min_x \sum_{i=1}^I \|T_i x\|_1 \quad \text{subject to} \quad F_u x = y \quad (4)$$

This is the proposed mathematical model in this Letter that combines sparsifying transforms for CS-MRI. It guarantees unbiased treatment of different transforms that sparsify images. In this Letter, a wavelet

that is good at representing point-like features and a contourlet that is good at representing curve-like features are employed as two fast transforms. An improved contourlet [6] is adopted because it has lower computing complexity [5,6] than a curvelet while approximating curves as well as a curvelet.

Because the acquired k-space data is often contaminated by noise in real applications, we solve the basis pursuit denoising problem as

$$\arg \min_x \frac{1}{2} \|F_u x - y\|_2^2 + \lambda \sum_{i=1}^I \|T_i x\|_1 \quad (5)$$

where  $\lambda$  trades off data consistency and sparsity. Large  $\lambda$  can suppress heavy noise.

Total variation (TV) is employed to assist the wavelet in [3]. Our combined transforms can also be associated with TV as

$$\arg \min_x \frac{1}{2} \|F_u x - y\|_2^2 + \lambda \sum_{i=1}^I \|T_i x\|_1 + \beta TV(x) \quad (6)$$

where  $\beta$  denotes the weight of TV.

The nonlinear conjugate gradient algorithm is employed as the numerical calculation for (5) and (6). We refer to the literature [3] for details but one must be aware of updating the solution according to (5) and (6).

**Stimulation results:** An MR image with fully sampled k-space data is acquired on a 1.5 Telsa GE MRI system. Ten per cent of k-space data is sampled according to the variable density sampling pattern [3] in Fig. 1a. We use the Daubechies wavelet with four decomposition levels and the contourlet with  $2^5, 2^4, 2^4, 2^3$  directional subbands from coarse to fine scales.  $\lambda$  is 0.0030 for single transform and 0.0015 for combined transforms to avoid affecting the performance of suppressing noise.

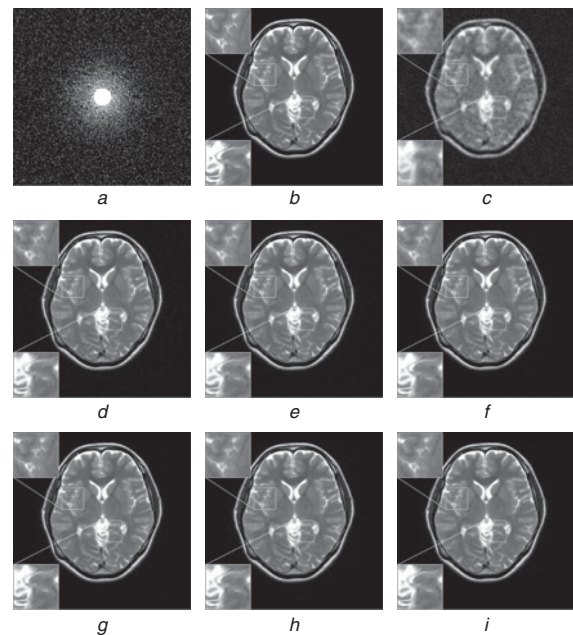


**Fig. 1** Sampling pattern and reconstructed images

a Sampling pattern with 10% of k-space data sampled  
b–c Reconstructed images from fully sampled and zero-filling k-space, respectively  
d–f Reconstructed images of wavelet, contourlet and combined sparsifying transforms without TV  
g–i Reconstructed images of wavelet, contourlet and combined sparsifying transforms with TV

Fig. 1d shows that the wavelet induces square-like artefacts and the curves are bad. Fig. 1e shows that the contourlet induces curve-like artefacts and loses the point feature. Fig. 1f shows the combined transforms can efficiently suppress both of the artefacts and improve the quality of reconstructed images. The point and curve features are simultaneously reconstructed well.

Because TV is well known for enforcing images to be piecewise constant, it is reasonable to use small  $\beta$  to avoid removing textures and oscillatory structures of MR images. In simulation, TV weight is  $5 \times 10^{-4}$ . With single transform, small TV weight cannot suppress the

artefact very well, as shown in Figs. 1g and h. However, the same weight is sufficient for combined transforms because few artefacts exist, as shown in Fig. 1i. In fact, we observe an obvious piecewise constant for both single and combined transforms when TV weight is larger than  $1 \times 10^{-3}$ .

Besides the visual appearance, power signal-to-noise ratio (PSNR) and transferred edge information (TEI) [8] serve as objective criteria. The PSNR is defined as

$$PSNR = 20 \log_{10} \left( \frac{255}{\sqrt{MSE}} \right) \quad (7)$$

where  $MSE = \frac{1}{P \times Q} \sum_{p=1}^P \sum_{q=1}^Q (\tilde{x}(p, q) - \hat{x}(p, q))^2$  and  $(p, q)$  is the pixel location of a  $P \times Q$  image.  $\hat{x}$  is the reconstructed image using CS-MRI and  $\tilde{x}$  is the reconstructed image from fully sampled k-space data. PSNR evaluates the difference in grey values between  $\hat{x}$  and  $\tilde{x}$ . TEI computes the edge information that  $\hat{x}$  has inherited from  $\tilde{x}$ .

Table 1 shows that combined transforms are obviously superior to a single transform without TV. When TV is added, combined transforms maintain an advantage over single transform though the improvement on single transform can be higher than combined transforms. It is demonstrated that combined transforms can perform well with small TV.

**Table 1:** Comparison of objective criteria for sparsifying transforms

	PSNR	TEI
Zero-filled	24.2	0.250
Wavelet	31.6	0.564
Contourlet	32.9	0.648
Combined transforms	34.7	0.675
Wavelet + TV	34.4	0.648
Contourlet + TV	34.4	0.668
Combined transforms + TV	35.7	0.691

When using different MR images and sampling patterns, analogous results of combined transforms with and without TV are still observed in terms of visual quality and objective criteria.

**Conclusion:** Combining wavelet and contourlet can simultaneously recover the point-like and curve-like image features. The combined

sparsifying transforms can improve the reconstruction quality of MR images from undersampled k-space data. For future work, the theoretical work on applying combined transforms for CS is to be considered to guide the reconstruction of images with plentiful features that the single transform cannot sparsely represent.

**Acknowledgment:** This work was partially supported by NNSF of China under grants 10774125 and 10605019.

© The Institution of Engineering and Technology 2010

28 June 2009

doi: 10.1049/el.2010.1845

X. Qu, X. Cao, D. Guo, C. Hu and Z. Chen (*Departments of Communication Engineering, Software Engineering, and Physics, Fujian Key Laboratory of Plasma and Magnetic Resonance, Xiamen University, Xiamen 361005, People's Republic of China*)

E-mail: chenz@xmu.edu.cn

## References

- 1 Candès, E., Romberg, J., and Tao, T.: 'Robust uncertainty principles: exact signal reconstruction from highly incomplete frequency information', *IEEE Trans. Inf. Theory*, 2006, **52**, (2), pp. 489–509
- 2 Donoho, D.: 'Compressed sensing', *IEEE Trans. Inf. Theory*, 2006, **52**, (2), pp. 1289–1306
- 3 Lustig, M., Donoho, D., and Pauly, J.M.: 'Sparse MRI: the application of compressed sensing for rapid MR imaging', *Magn. Reson. Med.*, 2007, **58**, (6), pp. 1182–1195
- 4 Candès, E., and Donoho, D.: 'Curvelets – a surprisingly effective nonadaptive representation for objects with edges', in Cohen, A., Rabut, C., Schumaker, L. (Eds.) 'Curves and surfaces' (Vanderbilt University Press, Nashville, TN, USA, 2000), pp. 105–120
- 5 Do, M.N., and Vetterli, M.: 'The contourlet transform: an efficient directional multiresolution image representation', *IEEE Trans. Image Process.*, 2005, **14**, (12), pp. 2091–2106
- 6 Lu, Y., and Do, M.N.: 'A new contourlet transform with sharp frequency localization'. 2006 Int. Conf. on Image Processing (ICIP 2006), Atlanta, GA, USA, 2006, pp. 1629–1632
- 7 Chen, S.B., Donoho, D., and Saunders, M.A.: 'Atomic decomposition by basis pursuit', *SIAM Rev.*, 2001, **43**, (1), pp. 129–159
- 8 Qu, G.H., Zhang, D.L., and Yan, P.: 'Information measure for performance of image fusion', *Electron. Lett.*, 2002, **38**, (7), pp. 313–315